A Design Methodology for a Dual-Mode Coplanar Waveguide Junction Circulator

Karthik Srinivasan

Electrical and Computer Engineering
Boise State University
Boise, ID, United States
karthiksrinivasa@boisestate.edu

Abstract— Circulators with inherent multiband operation are beneficial to low-power and small form factor radars for emerging beamforming and remote sensing applications. In this paper, a design methodology for a dual-mode junction circulator on coplanar waveguide structure is presented. Several magnetic and geometric parameters are shown to have an impact on the standing wave pattern at the circulator junction. Contrasting circulation directions are obtained at the two resonant frequencies of 4.76 GHz and 8.54 GHz with a low insertion loss of 1-2 dB and isolation ratios better than 35 dB and 22 dB for the first and second order modes, respectively.

Keywords—non-reciprocal devices, circulators, ferrites, full-duplex transceiver, multiband radars

I. INTRODUCTION

Junction circulators are 3-port ferrite-loaded devices that facilitate non-reciprocal transmission between a pair of adjacent ports while isolating the third port. Circulators are key to implementing full-duplex transceivers that transmit and receive over the same frequency band while avoiding selfinterference, transmitter coupling and leakage reception [1], [2]. Additionally, circulators have also been used to overcome RF phase circuit instabilities by separating the uplink and downlink beamforming networks in massive multiple-input multiple-output (MIMO) technologies [3]. Earliest models of a junction circulator presented by Bosma [4] and Fay and Comstock [5] consisted of two ferrite cylinders on either side of a stripline Y-junction with ground planes, as shown in Fig. 1(a). Two counter rotating normal modes are used to describe the circulator, which form a standing wave pattern (SWP) at the junction. The fundamental resonance mode, which has electric fields perpendicular and magnetic fields parallel to the junction plane, can be rotated in space by 30° under a DC magnetic bias to isolate one of the ports and facilitate nonreciprocal transmission between the other two ports [5]. As shown in Fig. 1(b), input signal from port 1 is routed to port 2 and port 3 remains isolated. Input to any other port will follow in the same circulation path because of symmetry, and the electric field null will align towards the isolated port.

Various implementations of circulators using stripline, microstrip and coplanar waveguides (CPW) have been reported in the literature for the S-, C- and X-bands. Notably, modelling efforts has shown stripline circulators loaded with Ni-Zn ferrite to have isolation ratios better than 40 dB and insertion loss < 1 dB [6], while fabricated microstrip circulators have resulted in an isolation ratio of 30 dB and insertion loss of ~1-2 dB [1], [7]. On the other hand, junction

Amal El-Ghazaly
Electrical and Computer Engineering
Cornell University
Ithaca, NY, United States
ase63@cornell.edu

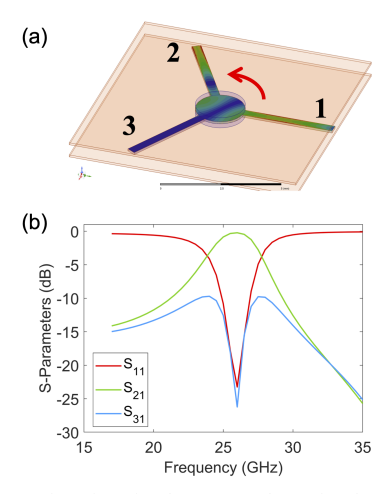


Fig. 1. A 3-port junction circulator. (a) Schematic of a stripline circulator with E-field standing wave pattern. (b) S-parameter plot with input in port 1 and output in port 2, while port 3 is isolated.

circulators in a CPW structure with varying thicknesses of yttrium iron garnet (YIG) [8], [9], have all shown isolation ratios exceeding 28 dB and insertion loss restricted to < 5 dB. However, these circulators are limited to operating in the fundamental resonance mode or n=1 mode, restricting them from accessing higher frequencies associated with n>1 modes. Circulators operating in higher-order modes will enable improved spectrum utilization through multi-band transceivers and have significant impact in advancing dual-band radars used in environmental monitoring [10], [11].

Typically, higher order modes are avoided in microwave components owing to their lossy characteristics and challenges in impedance matching, but some reports have shown promising dual-band operation in circulators. An early work by Razavipour et al. demonstrated a waveguide-based dual-frequency circulator that operated at 8.2 GHz and 10.4 GHz with an isolation ratio of 20 dB and insertion loss of 0.1 dB but required a large axially magnetized triangular ferrite rod [12]. Subsequently, Zhang et al. and Turki at al. reported in two separate instances a dual-band circulator, wherein the former required a tunable DC magnetic bias but could only achieve unidirectional circulation and the latter required an overlap of fundamental and higher order resonant modes for bidirectional circulation [13], [14]. In a more recent report, Olivier et al. provided a design criteria for modifying the frequency separation between the operating bands through eigenmode analysis and parametric sweep, but required geometric changes to reverse the circulation direction [15].

Bidirectionality can be useful in enabling hybrid dual band transceiver designs, where two single-band transceiver sections with a unidirectional circulator can access the same broadband antenna through a third bidirectional circulator [12]. Such implementations can also be expanded to realize power combiners in multiband radars or complex bandpass filtering transfer functions through cascaded bidirectional circulators [1]. In this work we demonstrate the design and modeling efforts in realizing a bidirectional dual-mode circulator in a CPW structure with integrated ferrite and without manual tuning. Specifically, parametric optimizations provide insights into expanding the demonstrated design for other frequencies in the Ku, K and Ka bands.

DESIGN OF A DUAL-MODE CIRCULATOR

The SWP at the junction contains RF magnetic fields that have a circular polarization in the center, which becomes increasingly elliptical away from center and results in a linear polarization at the edge. Under a DC magnetic bias, the resonant frequency splits and the direction of spin precession in the ferrite leads to different permeabilities for each of the counter-rotating modes. Considering the tensorial nature of the in-plane permeability, the Polder formalism can be used to define the permeability as,

$$|\mu| = \begin{vmatrix} \mu & j\kappa & 0 \\ -j\kappa & \mu & 0 \\ 0 & 0 & 1 \end{vmatrix}$$
 (1)

Where, the diagonal (μ) and off-diagonal (κ) components are,

$$\mu = 1 + \frac{\omega_z \omega_m}{\omega_z^2 - \omega^2} \tag{2}$$

$$\kappa = \frac{\omega \omega_{\rm m}}{\omega_{\rm r}^2 - \omega^2} \tag{3}$$

Here, ω_z and ω_m are defined as angular frequencies of the spin-precession that correspond to the internal DC magnetic field (H₀ in Oe) and saturation magnetization ($4\pi M_S$ in G) of the ferrite, respectively.

$$\omega_z = 2\pi \times 2.8 \times H_0 \times 10^6 \text{ rad/s} \tag{4}$$

$$\omega_{\rm m} = 2\pi \times 2.8 \times 4\pi M_{\rm S} \times 10^6 \,\text{rad/s} \tag{5}$$

Using (1) - (5), the components of the Polder tensor are calculated for a ferrite with a saturation magnetization of 900 G, an anisotropy field of 7 kOe, an external DC magnetic field of 100 Oe and a linewidth broadening from inhomogeneities (ΔH) of 500 Oe. These magnetic parameters along with the internal magnetic anisotropy field lead to induced internal DC magnetic field in the ferrite, which determines the resonant characteristics. These magnetic properties are typical of GdCo alloys or spin-on-ferrites with YIG nanoparticles [16], [17]. Other ferrites such as single crystal or polycrystalline garnet thin films may have higher saturation magnetization and narrower linewidths [18]. The dispersion plots for Polder parameters in Fig. 2(a) with an internal field (sum of anisotropy field and external bias field) of 7100 Oe shows a resonance near 20 GHz for the real (μ', κ') and imaginary (μ'',κ'') parts of the Polder tensor. After determining a suitable operating frequency, the radius of the circulator junction can be calculated based on the theory of circulation,

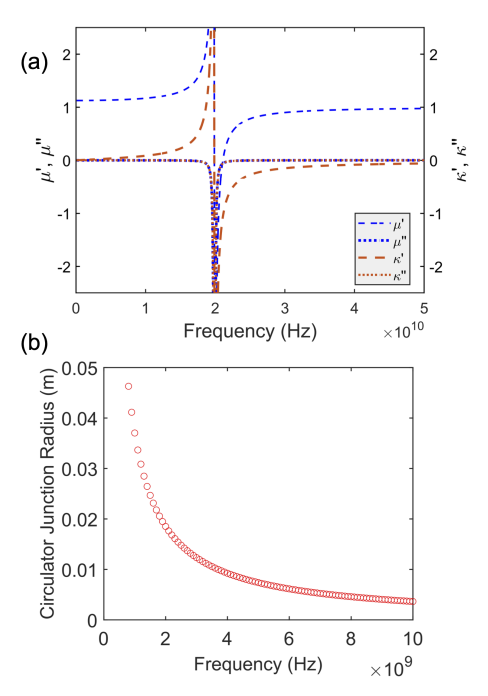


Fig. 2. (a) Real and imaginary parts of the diagonal (µ) and offdiagonal (κ) components of the Polder permeability tensor for a ferrite. (b) Radius of the circulator junction at various frequencies.

$$R = \frac{1.84}{\frac{\omega}{c} (\varepsilon_f \mu_{eff})^{1/2}} \tag{6}$$

Where, the effective permeability parameter is defined as,

$$\mu_{eff} = \frac{\mu^2 - \kappa^2}{\mu} \tag{7}$$

 $\mu_{eff} = \frac{\mu^2 - \kappa^2}{\mu} \tag{7}$ Consequently, using (6)-(7) and the plot shown in Fig. 2(b), the radius of the circulator for an operating frequency of 5 GHz is ~7 mm. Typically, the dimensions of the waveguides feeding to the circulator junction are a quarter-wave impedance transformer to provide impedance matching with the feed line or load. However, this cannot be applied for dualmode circulators as the impedance characteristics change significantly between the two frequencies. One alternative is to design the two resonant modes to be closely spaced in frequency of operation, but this degrades isolation characteristics. In this work, the CPW is designed to provide impedance matching at n = 1, while a small trade-off between isolation ratio and return loss is tolerated at the higher-order mode.

III. RESULTS AND DISCUSSION

The CPW junction circulator shown in Fig. 3(a) is designed with the geometrical, electrical and magnetic parameters shown in Table 1. Fig. 3(b) shows the S-parameter plot from Ansys HFSS simulations, which shows two distinct resonances at 4.76 GHz (f₁) and 8.54 GHz (f₂), which correspond to the first- and second-order modes. However, the isolation ratios at f₁ and f₂ are only 12 dB and 8 dB, respectively, with an insertion loss of 2-3 dB across both bands. A closer look at the E-field map at the junction shows limited power transfer between the input and output ports. Circulator theory from Fay and Comstock suggests that for effective isolation, the SWP must be rotated by 30°, which

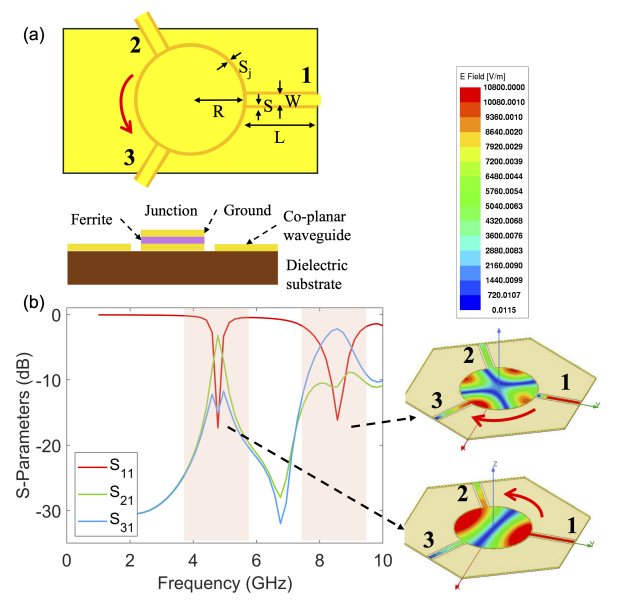


Fig. 3. (a) Schematic illustration of a CPW circulator. (b) S-parameters describing dual-mode circulation at 4.76 GHz (f_1) and 8.54 GHz (f_2) , corresponding to the first and second-order modes, respectively. At f_1 , circulation is counter-clockwise and E-field null is off-centered from the isolated port 3. At f_2 , clockwise circulation isolates port 2.

corresponds to a 30° phase angle of the impedances for the two counter-rotating first-order modes [5]. Such geometric rotations are possible by changing the internal DC magnetic field. At f_1 , the E-field null is off-centered away from the isolated port, indicating excess external magnetic field. In the case of second-order mode at f_2 , even though the geometric rotation of standing waves needed is only 15° (because of 2 cycles around the disk), the isolation ratio is also affected by poor impedance matching of the coplanar structure.

Table I. Geometric, Electrical and Magnetic Design Parameters^a

R	S	S_j	W	L	t _e
6.9 mm	360 μm	150 μm	1 mm	8.28 mm	35 μm
t _m	t_{sub}	H_0	$4\pi M_s$	$\epsilon_{ m d}$	ε _f
50 μm	203 μm	7100 G	900 G	3.28	5.7

 ^{a}R – Junction radius, S – CPW gap, S_{j} – CPW junction gap, W – CPW width, L – CPW length, t_{e} – Electrode thickness, t_{m} – Ferrite thickness, t_{sub} – Substrate thickness, ϵ_{d} – Substrate permittivity, ϵ_{f} – Ferrite permittivity

Design changes to geometrically rotate the SWP at f₁ and impedance match at f2 requires a reconsideration of the external DC magnetic bias and CPW structure. Circulator mode dispersion from [5] suggests that dual-band circulation at n = 1 and n = 2 can be obtained in a small external magnetic field. However, this study considers ferrites with strong anisotropy and circulation below ferromagnetic resonance, which places the operating point in the high-field regime [15]. Therefore, reducing the anisotropy field without changing the external bias should decrease the internal magnetic field and compensate the excess geometric rotation of the SWP. Next. geometric parametric sweeps varying the waveguide length, CPW gap and CPW junction gap were carried out to identify their impact on isolation ratio and insertion loss. The waveguide length was varied from 6-18 mm and an optimal length of 8.28 mm was identified for a large isolation ratio at f₁. This substantiates the previously discussed design based on a quarter wavelength for the CPW feed waveguide. As noted before, quarter wavelength design cannot be applied for both f_1 and f_2 in the same physical device, leading to a trade-off at f_2 . Fig. 4(a) and 4(b) show results from the co-optimization of CPW gap for the feed waveguide and circulator junction, which results in optimal values of 150 μm and 100 μm , respectively. In all cases, the insertion loss was between 1-2 dB and did not show meaningful variations. Similarly, as shown in Fig. 4(c) a waveguide width (W) of at least 900 μm resulted in a large isolation ratio and low return loss for all simulated dimensions up to 1500 μm .

Based on the results of the parametric sweep, the geometric parameters were updated, and the internal DC magnetic field was reduced to 5025 G in the modified circulator design. S-parameter plot in Fig. 5(a) shows improved dual-mode circulation characteristics with expected resonances at f₁ and f₂. The isolation ratio and insertion loss are 35 dB and 2.4 dB (at f₁), and 22 dB and 1.5 dB (at f₂), respectively. E-field maps at the two resonant frequencies indicate a counter-clockwise circulation at f₁ and clockwise circulation at f₂. This is reversed if the direction of external DC magnetic bias is also reversed. It is also noted that the E-field and H-field components of the simulated design form a dipolar mode as expected from the theoretical predictions for a junction circulator as shown in Fig. 5(b). While the E-field map has been described previously, the direction of E-field

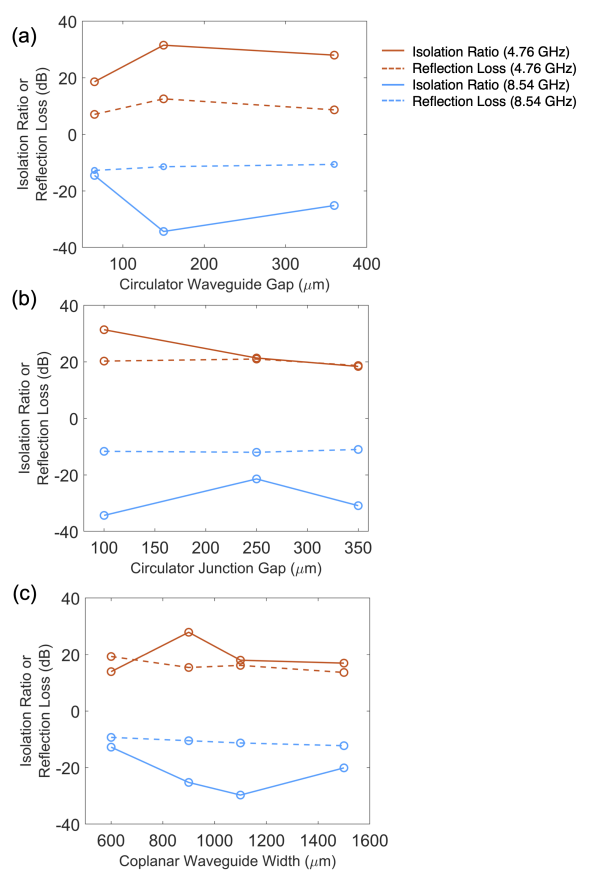


Fig. 4. Parametric optimization of isolation ratio and reflection loss for various geometric design parameters. (a) CPW gap. (b) Circulator junction gap. (c) CPW width.

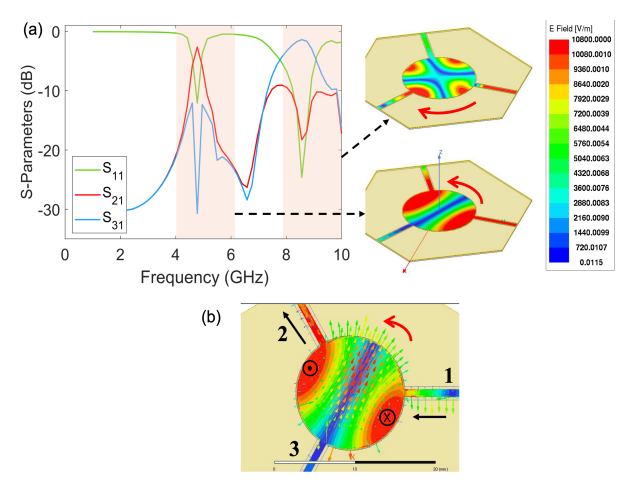


Fig. 5. Optimized dual-mode CPW circulator. (a) S-Parameters and E-field SWP at resonant frequencies 4.76 GHz and 8.54 GHz with bidirectional circulation. (b) E-field (colormap) and H-field (arrows) in the junction demonstrate a dipolar mode consistent with theory.

vector is normal to the junction plane and the H-field vectors are parallel to the junction surface. Although the circulator shown here operates in the C and X band, this design can be readily modified for operation in other frequency bands extending up to millimeter waves in the K and Ka bands.

IV. SUMMARY

This paper presents a design methodology for a dual-mode CPW circulator, wherein the same physical device can simultaneously circulate electromagnetic waves at two distinct frequencies. A thorough design process is presented which considers several geometric, electrical and magnetic parameters that impact the different resonant modes of the circulator. Specifically, geometric and magnetic parameters that caused impedance and mode-geometry mismatch at the two operating frequencies were identified and optimized. Isolation ratios better than 35 dB and 20 dB are achieved for the first and second-order modes, respectively, while the insertion losses are as low as 1-2 dB. Unlike other multi-band circulators, the designs demonstrated here do not require manual tuning of an external magnetic bias or engineering of complex modes to facilitate multi-band transmission. Circulators with inherent multi-band behavior will have a significant impact to enabling low-power and small form factor dual-band radars integrated with a broadband antenna.

ACKNOWLEDGMENT

This material is based upon work supported by the National Science Foundation (NSF) under Grant No. 2030207. Any opinions, findings, and conclusions or recommendations expressed in this material are those of the authors and do not necessarily reflect the views of the NSF.

REFERENCES

- [1] A. Ashley and D. Psychogiou, "Ferrite-Based Multiport Circulators With RF Co-Designed Bandpass Filtering Capabilities," *IEEE Trans. Microw. Theory Tech.*, vol. 71, no. 6, pp. 2594–2605, Jun. 2023, doi: 10.1109/TMTT.2022.3233630.
- [2] N. Reiskarimian, M. B. Dastjerdi, J. Zhou, and H. Krishnaswamy, "Analysis and Design of Commutation-Based Circulator-Receivers for

- Integrated Full-Duplex Wireless," *IEEE J. Solid-State Circuits*, vol. 53, no. 8, pp. 2190–2201, Aug. 2018, doi: 10.1109/JSSC.2018.2828827.
- [3] H.-T. Chou, C.-H. Chang, and Y.-T. Chen, "Ferrite Circulator Integrated Phased-Array Antenna Module for Dual-Link Beamforming at Millimeter Frequencies," *IEEE Trans. Antennas Propag.*, vol. 66, no. 11, pp. 5934–5942, Nov. 2018, doi: 10.1109/TAP.2018.2862343.
- [4] H. Bosma, "On the principle of stripline circulation," *Proc. IEE Part B Electron. Commun. Eng.*, vol. 109, no. 21S, pp. 137–146, Jan. 1962, doi: 10.1049/pi-b-2.1962.0027.
- [5] C. E. Fay and R. L. Comstock, "Operation of the Ferrite Junction Circulator," *IEEE Trans. Microw. Theory Tech.*, vol. 13, no. 1, pp. 15– 27, Jan. 1965, doi: 10.1109/TMTT.1965.1125923.
- [6] A. Setiawan, Y. Y. Maulana, Y. Sulaeman, T. Praludi, and Y. Taryana, "Design of 3 GHz stripline ferrite circulator for radar applications," in 2017 International Conference on Radar, Antenna, Microwave, Electronics, and Telecommunications (ICRAMET), Jakarta: IEEE, Oct. 2017, pp. 154–157. doi: 10.1109/ICRAMET.2017.8253166.
- [7] A. Ashley, L. F. Marzall, M. Pinto, Z. Popovic, and D. Psychogiou, "Bandwidth design of ferrite-based circulators," in 2018 International Applied Computational Electromagnetics Society Symposium (ACES), Denver, CO: IEEE, Mar. 2018, pp. 1–2. doi: 10.23919/ROPACES.2018.8364118.
- [8] K. Oshiro et al., "Fabrication of circulator with coplanar wave guide structure," *IEEE Trans. Magn.*, vol. 41, no. 10, pp. 3550–3552, Oct. 2005, doi: 10.1109/TMAG.2005.854729.
- [9] O. Zahwe, B. Sauviac, and J. J. Rousseau, "FABRICATION AND MEASUREMENT OF A COPLANAR CIRCULATOR WITH 65 μm YIG THIN FILM," Prog. Electromagn. Res. Lett., vol. 8, pp. 35–41, 2009, doi: 10.2528/PIERL09030604.
- [10] R. J. Chase, S. W. Nesbitt, and G. M. McFarquhar, "A Dual-Frequency Radar Retrieval of Two Parameters of the Snowfall Particle Size Distribution Using a Neural Network," Mar. 2021, doi: 10.1175/JAMC-D-20-0177.1.
- [11] R. Willatt et al., "Retrieval of Snow Depth on Arctic Sea Ice From Surface-Based, Polarimetric, Dual-Frequency Radar Altimetry," Geophys. Res. Lett., vol. 50, no. 20, p. e2023GL104461, 2023, doi: 10.1029/2023GL104461.
- [12] H. Razavipour, G. Askari, F. Fesharaki, and H. Mirmohammad-Sadeghi, "A new high-power, dual-band, E-plane, ferrite circulator," in *IEEE EUROCON 2009*, St. Petersburg, Russia: IEEE, May 2009, pp. 20–25. doi: 10.1109/EURCON.2009.5167598.
- [13] Yuanyuan Zhang, Xixi Feng, Kaiqiang Zhu, Xi Yang, and Houmin Li, "An X-band tunable circulator based on Yttrium iron garnet thin film," in 2016 IEEE International Conference on Microwave and Millimeter Wave Technology (ICMMT), Beijing, China: IEEE, Jun. 2016, pp. 425–427. doi: 10.1109/ICMMT.2016.7761796.
- [14] H. Turki, L. Huitema, T. Monediere, B. Lenoir, and C. Breuil, "New Concept Validation of Low-Loss Dual-Band Stripline Circulator," *IEEE Trans. Microw. Theory Tech.*, vol. 67, no. 3, pp. 845–850, Mar. 2019, doi: 10.1109/TMTT.2018.2890632.
- [15] V. Olivier et al., "Dual-Band Ferrite Circulators Operating on Weak Field Conditions: Design Methodology and Bandwidths' Improvement," *IEEE Trans. Microw. Theory Tech.*, vol. 68, no. 7, pp. 2521–2530, Jul. 2020, doi: 10.1109/TMTT.2020.2988003.
- [16] K. Srinivasan and A. El-Ghazaly, "Tunable Non-Reciprocal Phase Shifter and Spin-Coated Ferrites for Adaptive Microwave Circuits," in 2023 International Microwave and Antenna Symposium (IMAS), Cairo, Egypt: IEEE, Feb. 2023, pp. 62–65. doi: 10.1109/IMAS55807.2023.10066899.
- [17] K. Srinivasan, Y. Chen, L. Cestarollo, D. K. Dare, J. G. Wright, and A. El-Ghazaly, "Engineering large perpendicular magnetic anisotropy in amorphous ferrimagnetic gadolinium cobalt alloys," *J. Mater. Chem. C*, vol. 11, no. 14, pp. 4820–4829, Apr. 2023, doi: 10.1039/D3TC00332A.
- [18] T. Qu et al., "Nonlinear Magnon Scattering Mechanism for Microwave Pumping in Magnetic Films," *IEEE Access*, pp. 1–1, 2020, doi: 10.1109/ACCESS.2020.3040711.